Available online at www.sciencedirect.com
SCIENCE DIRECT®
Journal of Molecular Catalysis A: Chemical 209 (2004) 107–115
JOURNAL OF MOLECULAR CATALYSIS A: CHEMICAL
www.elsevier.com/locate/molcata

# Pd/NaY-zeolite and Pd-W/NaY-zeolite catalysts: preparation, characterization and NO decomposition activity

Sibele B.C. Pergher [a], Rogério M. Dallago [a,d], Renato Cataluña Veses [b], Carlos E. Gigola [c], Ione M. Baibich [b,*]

[a] *Departamento de Química, URI, Campus Erechim, Av. Sete de Setembro, 1621, CEP 99700-000, Erechim, RS, Brazil*
[b] *Instituto de Química, UFRGS, Av. Bento Gonçalves, 9500, CEP 91501-970, Porto Alegre, RS, Brazil*
[c] *PLAPIQUI, Km 7 Camino "La Carrindanga" C.C. 717-8000, Bahia Blanca, Argentina*
[d] *Intituto de Química, UCS, Francisco Getúlio Vargas, 1130, Caxias do Sul, RS, CEP 95070-560, Brazil*

Received 28 April 2003; received in revised form 7 August 2003; accepted 11 August 2003

**Abstract**

In this work, Pd/NaY-zeolite and Pd-W/NaY-zeolite catalysts were prepared from the compounds $Pd(NO_3)_2$ and $[W(CO)_6]$. Palladium catalysts supported on NaY-zeolite were prepared by ion exchange and impregnation methods. Subsequently, tungsten was added by photochemical activation of $[W(CO)_6]$ in order to obtain a Pd-W interaction. The catalysis materials were characterized by diffuse reflectance (DRIFTS)–FTIR, chemical analysis (AAS), temperature programmed reduction (TPR), X-ray diffraction (XRD), $H_2$ chemisorption and sorption measurements. The prepared catalysts were found to be active for NO decomposition at 573 K leading mainly to $N_2$ and $N_2O$. The conversion of NO and the selectivity to $N_2O$ were studied as a function of time and the reduction temperature. The Pd/NaY-zeolite and the Pd-W/NaY-zeolite samples exhibited an initial period of high and constant activity followed by deactivation. For samples reduced at 573 K the deactivation process becomes more pronounced in the presence of tungsten. On the other hand when the reduction pretreatment was carried out at 973 K the presence of tungsten allowed the catalysts to have a higher conversion for a longer period of time. Tungsten prevents the sintering of small palladium particles. Another beneficial effect of tungsten was a significant suppression of $N_2O$ formation. The selectivity for $N_2O$ at similar NO conversion level was lower on Pd-W/NaY-zeolite.


*Keywords:* NO decomposition; NaY-zeolite; Palladium; Tungstencarbonyl; Catalysts

## 1. Introduction

In an attempt to increase the catalytic activity of palladium catalysts for the removal of hydrocarbons and $NO_x$ several promoters such as $WO_3$, $Co_3O_4$, $La_2O_3$ and $MO_3$ have been used [1–9]. The interaction between the noble metal and the oxide seems to be an essential condition for changing the catalytic behavior. However, using inorganic precursors a high metal oxide loading is in fact needed to satisfy this condition. One way of preventing this problem is the use of organometallic compounds; in this way preparations with low loadings and more controlled interactions could be obtained.

Recently, we have demonstrated that an alternative procedure for depositing tungsten or molybdenum on $Al_2O_3$ or $Pd/Al_2O_3$ is based on the photochemical reaction of $[M(CO)_6]$ compounds (M = W, Mo) [10–14]. In this way we have prepared and characterized catalysts where tungsten or molybdenum were found in close association with palladium. Moreover, these catalysts showed high activity for NO decomposition [12,15].

The purpose of this work was to extend our previous studies performed on γ-$Al_2O_3$ to zeolites, as it is known that metalcarbonyls interact more strongly with zeolites that with alumina [16–19]. Another motivation for this work are the reports that show that very active and selective catalysts for the reduction of nitric oxide with methane are obtained by supporting palladium on zeolites [20,21], the role of the support being the stabilization of $Pd^{2+}$ species. Hence, Pd/NaY-zeolite catalysts were prepared by dry impregnation and ionic exchange methods and the related

* Corresponding author. Tel.: +55-51-333-30414; fax: +55-51-331-66304.
*E-mail address:* ione@iq.ufrgs.br (I.M. Baibich).

1381-1169/$ – see front matter © 2003 Elsevier B.V. All rights reserved.
doi:10.1016/j.molcata.2003.08.005

Pd-W/NaY-zeolite catalysts were obtained by photochemical activation of $[W(CO)_6]$. A high amount of Pd was incorporated on the support by the ionic exchange method, in the hope of increasing the interaction with tungsten, since it is known that metalcarbonyls react preferentially with large palladium particles [13]. The monometallic and bimetallic catalysts were characterized by hydrogen sorption, chemisorption and temperature programmed reduction (TPR) measurements. In addition, the effect of tungsten on the activity and selectivity of Pd/NaY-zeolite for NO decomposition at 573 K was investigated for samples reduced at 573 and 973 K.

## 2. Experimental

The catalysts were prepared using a commercial NaY-zeolite as a support. The NaY-zeolite was obtained from ITQ, Valencia, Spain (surface area 655 $m^2/g$; $SiO_2/Al_2O_3 = 5.2$ and $Na_2O/Al_2O_3 = 1.02$ molar ratio).

The NaY-zeolite has a structure that shows two channel systems interconnected. One system was formed by the union of α supercages (i.d. = 12.4 Å) that can be reached by channels 12 membered rings (12 MR) with a diameter of 7.8 Å. Another channel system is formed by the alternated connection of sodalite cages (i.d. of 6.6 Å) and the α supercage, that can be reached by channels 6 MR (diameter of 2.2 Å).

The NaY-zeolite support was first treated in synthetic air for 3 h at 723 K and under vacuum for 1 h at 723 K. The material was cooled at room temperature in vacuum and then stored under argon.

### 2.1. Pd incorporation

In the pretreated support, palladium was incorporated by two different methods: ionic exchange (IE) and dry impregnation (DI), following the procedure described by Cañizares et al. [22].

In the ionic exchange method, a $Pd(NO_3)_2$ solution (20 ml of 0.05 mol/l for 1 g of support) was added in a pretreated support at 298 K and under agitation for 2 h. Then, the suspension was filtered and washed with deionizated water.

In the dry impregnation method, a specific quantity of $Pd(NO_3)_2$ solution was added in a pretreated support. The quantity used, equal to the pore volume of the support material was calculated to place approximately 1% of palladium by weight on the support. The solvent was removed by evaporation.

The samples prepared by both methods were dried at 393 K for 14 h, and treated at 673 K in synthetic air for 3 h and then reduced with $H_2$ at 573 or 973 K for 1 h.

### 2.2. W incorporation

The W incorporation was carried out through a photochemical activation of the organometallic compound $[W(CO)_6]$ (Aldrich) and hexane as solvent in the presence of the Pd/NaY-zeolite catalyst. The quantities used were calculated to give 2% by weight of W on the zeolite (1 g of Pd-zeolite; 0.038 g of $[W(CO)_6]$; 40 $cm^3$ of hexane).

The photochemical reactions were performed at room temperature under an Ar atmosphere using a Philips HPL-N (125 W) UV lamp fitted into a Pyrex cold finger. In order to observe the reaction progress, small liquid samples were withdrawn for analysis by FTIR. After an irradiation time of 6 h, the solid was filtered and washed with hexane. Small amounts of solution were removed for solution FTIR analysis.

Finally, the generated subcarbonyl species were decomposed by thermal treatment at 573 K under vacuum.

### 2.3. Characterization

The prepared materials were characterized by DRIFTS–FTIR, chemical analysis (AAS), temperature programmed reduction (TPR), X-ray diffraction (XRD) and $H_2$ chemisorption and sorption experiments. Diffuse reflectance (DRIFTS) spectra were recorded at ca. 293 K on a Bomem MB-102 Spectrometer, coadding 32 scans at a resolution of 4 $cm^{-1}$. The study was restricted to the $\nu$(CO) region (2200–1700 $cm^{-1}$). The solid phases were analyzed as powder in a DRIFTS accessory, equipped with sampling cups. The latter were filled with the support powder and transferred to the equipment as fast as possible, to prevent decomposition. These spectra were collected as reflectance units and transformed to Kubelka–Munk (KM) units. The solutions were analyzed with a pair of matched NaCl solution cells (0.10 mm pathlengths).

The TPR experiments were carried out in a conventional apparatus using an $H_2$/Ar mixture (5% $H_2$). Catalysts samples of 20 or 100 mg, depending on the metal content, were packed in a glass tube and pretreated in a flow of 4.9% $O_2$/Ar at 773 K for 1 h. After oxygen treatment, the samples were purged under a flow of argon and then cooled to 223 K. The TPR profiles were obtained in the 223–773 K temperature range with a heating rate of 10 K/min at a constant flow rate of 20 $cm^3$/min.

Hydrogen chemisorption and sorption isotherms were measured in a volumetric glass adsorption apparatus equipped with a MKS Baratron type PDR-A pressure gauge. An ultimate vacuum near $9.3 \times 10^{-4}$ Pa could be obtained, as measured by a Granville-Philips Model 274002 ionization gauge. The amount of hydrogen absorbed and chemisorbed on the exposed palladium atoms was measured after sample reduction in flowing $H_2$ at 573 K followed by overnight evacuation at the same temperature and cooling to room temperature. Subsequently, the amount of absorbed hydrogen forming α or β palladium-hydride was measured after room temperature evacuation for 30 min. In this way, only the amount of absorbed hydrogen is removed while that corresponding to strongly chemisorbed hydrogen, $(H/Pd)_s$, remains on the surface [23]. Unfortunately, reliable measurements of this

amount of hydrogen, which provides information on the fraction of exposed palladium atoms, was only possible for the Pd-W/NaY (DI) sample due to the unavailability of the appropriate amount of the Pd/NaY (DI) catalyst and the very small metal dispersion (large particles) on the catalysts prepared by ionic exchange. Consequently, on samples with high metal loading the palladium particle size was measured by X-ray diffraction line broadening. Experiments were performed on a Siemens D 5000 instrument operated at 30 kV and 30 mA with radiation from a Cu target. The particle size was calculated by the Scherrer equation with the peak width corresponding to the Pd (1 1 1) reflection.

### 2.4. Catalytic activity

The catalytic activity for NO decomposition of the prepared catalysts was measured in a glass flow reactor (i.d. = 13 mm) coupled to a FTIR MB100-BOMEM spectrometer equipped with a multiple-reflexion gas cell (7.0 m path length and 2.1 l volume). The reaction was studied as a function of time at 573 K, using a feed mixture of NO (500 ppm) in Ar. The glass reactor was filled with 120 mg of catalyst and the flow rate was adjusted at 60 $cm^3$/min. The NO, $NO_2$ and $N_2O$ stretching bands were monitored. The bands intervals were 1955–1790 $cm^{-1}$, 1658–1565 $cm^{-1}$ and 2266–2159 $cm^{-1}$, respectively. In order to calculate the NO conversion from the IR data a method developed in our laboratory by Dallago et al. [24] was used. It enables us to determine with precision the NO concentration at the entrance of the gas cell (reactor exit) from the absorbance values measured.

## 3. Results and discussion

The main properties of the mono and bimetallic catalysts are presented in Table 1. The very large palladium uptake shown by the sample prepared by IE, 8.9%, is in accord with the use of a concentrated solution of $Pd(NO_3)_2$. Taking into account that the NaY-zeolite has a Si/Al ratio of around 2.4, the amount of palladium corresponds to an exchange capacity of about 38%. Due to the high metal loading the palladium particle size measured by XRD on the monometallic and the bimetallic sample was quite large; 32–33 nm. On the other hand, using the DI method a palladium sample with a much lower metal uptake was obtained; 1.26%. We were able to perform a hydrogen chemisorption measurement on the bimetallic sample and the $(H/Pd)_s$ ratio that is equal to the fraction of exposed palladium atoms was found to be 0.25. Using this value the palladium particle size was estimated from the equation: $d$ (nm) = $1.12/(H/Pd)_s = 4.5$ as shown in Table 1 [25]. Taking into account that the chemisorption measurement was carried out on the bimetallic sample, the palladium particle size may be smaller if W atoms are deposited on the metal surface precluding the adsorption of hydrogen.

Table 1
Main catalyst properties

| Catalysts | Pd (wt.%)[a] | W (wt.%)[b] | Pd particle size (nm) |
|---|---|---|---|
| Pd/NaY (IE) | 8.9 | – | 33[c] |
| Pd/NaY (DI) | 1.26 | – | – |
| Pd-W/NaY (IE) | 8.9 | 1.9 | 32[c] |
| Pd-W/NaY (DI) | 1.26 | 1.6 | 4.5[d] |

IE: Pd incorporation by ionic exchange; DI: Pd incorporation by dry impregnation.

[a] Determined by AAS.

[b] From the decrease of the $\nu$(CO) IR band of $W(CO)_6$ in hexane solution.

[c] From XRD line broadening.

[d] From $H_2$ chemisorption; $d$ (nm) = $1.12/(H/Pd)_s$.

### 3.1. Pd/ NaY-zeolite catalysts

The TPR profiles of the two Pd/NaY-zeolite catalysts are shown in Fig. 1. It is important to notice that the mass of catalyst used in each experiment was varied in order to compensate for the large difference in metal content. The low temperature peaks in these profiles are clearly due to the reduction of palladium oxide crystals and β-hydride formation. The subsequent negative peaks are due to hydrogen desorption (β-hydride decomposition). The sample prepared by ion exchange shows a much higher hydrogen uptake, the reduction temperature is the lowest, 269 K and the peak due to hydrogen desorption at 347 K is very sharp. This behavior, which is typical of preparations with a low metal dispersion (large particles), is due to the high palladium concentration. Homeyer and Sachtler [26] have reported similar TPR profiles for 2% Pd/NaY sample prepared by IE following oxidation at 773 K. The presence of large palladium particles on the Pd/NaY (IE) sample, demonstrated by the XRD measurements, was confirmed by the $H_2$ sorption data. As shown in Fig. 2 the α-hydride phase to β-hydride phase transition is quite sharp.

On the other hand, the catalyst prepared by DI shows a TPR profile with a higher reduction temperature, 295 K, the peak is broader and the hydrogen desorption peak is located at a higher temperature; 351 K. Due to the lower metal loading, there is a stronger interaction with the zeolite leading to small particles. In other words, the palladium dispersion is much higher. In accordance with this situation the hydrogen sorption results in Fig. 2 demonstrate the absence of the α–β-hydride transition. It is important to realize that the hydrogen uptakes in Fig. 2 correspond to the amount absorbed, $(H/Pd)_{abs}$, not to hydrogen adsorbed. Extrapolation to zero pressure gives the amount of hydrogen due to the α-hydride phase which is equal for both samples, as expected. On the other hand, extrapolation of the high pressure region for sample Pd/NaY(IE) gives a value of $(H/Pd)_{abs} = 0.65$ which is close to the palladium-hydride stoichiometry for the β-hydride phase [27].

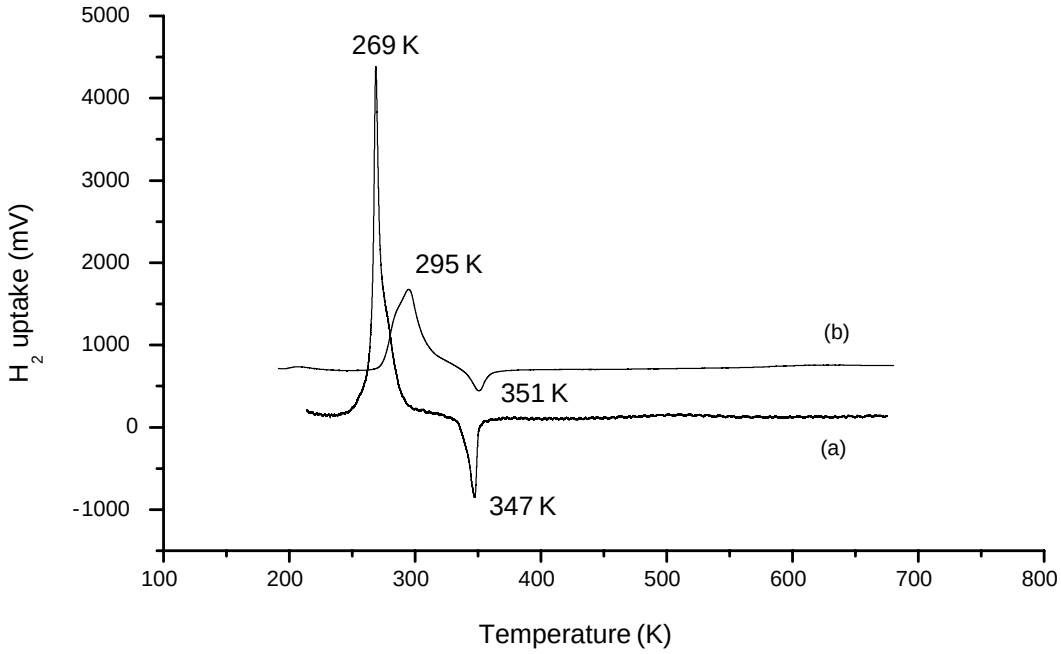


Fig. 1. TPR profiles of Pd/NaY (IE), $m = 100$ mg (a) and Pd/NaY (DI), $m = 20$ mg (b) following oxidation in $O_2$/Ar at 773 K.

### 3.2. Pd-W/NaY-zeolite catalysts

The amount of tungsten incorporated on the Pd/NaY-zeolite samples was followed by the decrease of the $\nu$(CO) IR band of $[W(CO)_6]$ (1983 $cm^{-1}$) in the hexane solution, as it has been explained elsewhere [10–14]. As shown in Table 1 the tungsten loading does not depend on the amount of palladium; it was slightly higher in the ion exchange preparation.

After the photochemical reaction, the DRIFTS spectra of the solid did not show any $\nu$(CO) band, in opposition to the situation where a ligand ($PPh_3$) was used to stabilize the tungstencarbonyl derivatives [10,11]. The beneficial effect of this ligand in stabilizing surface species on NaY-zeolite is shown in Fig. 3a. This spectrum is more complex than the one obtained when the same reaction was performed on alumina [12]. The bands might be attributed to either a

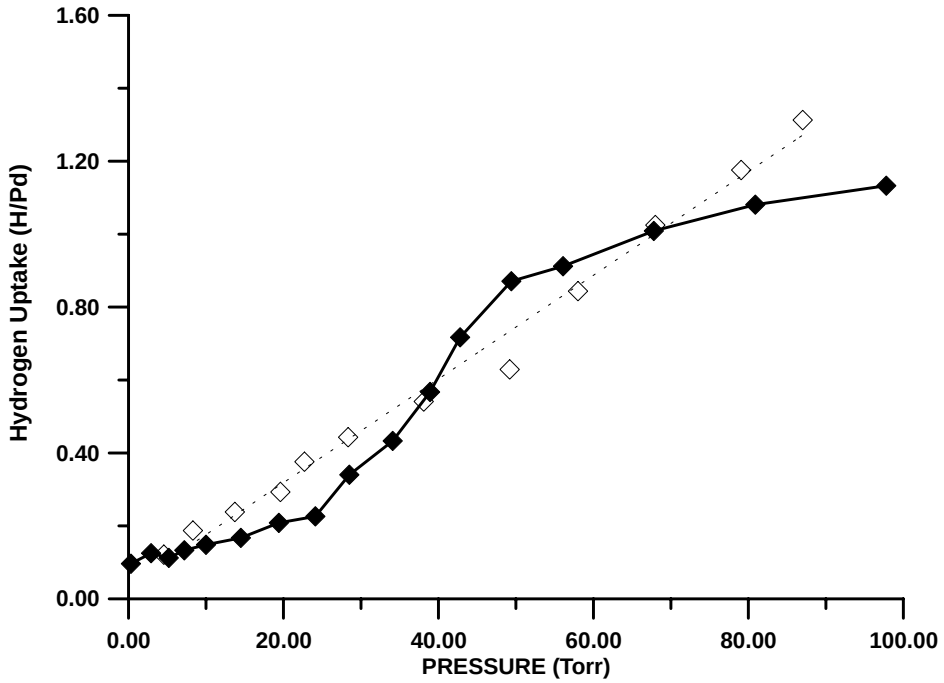


Fig. 2. Hydrogen sorption vs. pressure for Pd/NaY (IE) (◆) and Pd/NaY (DI) (□) at 308 K.

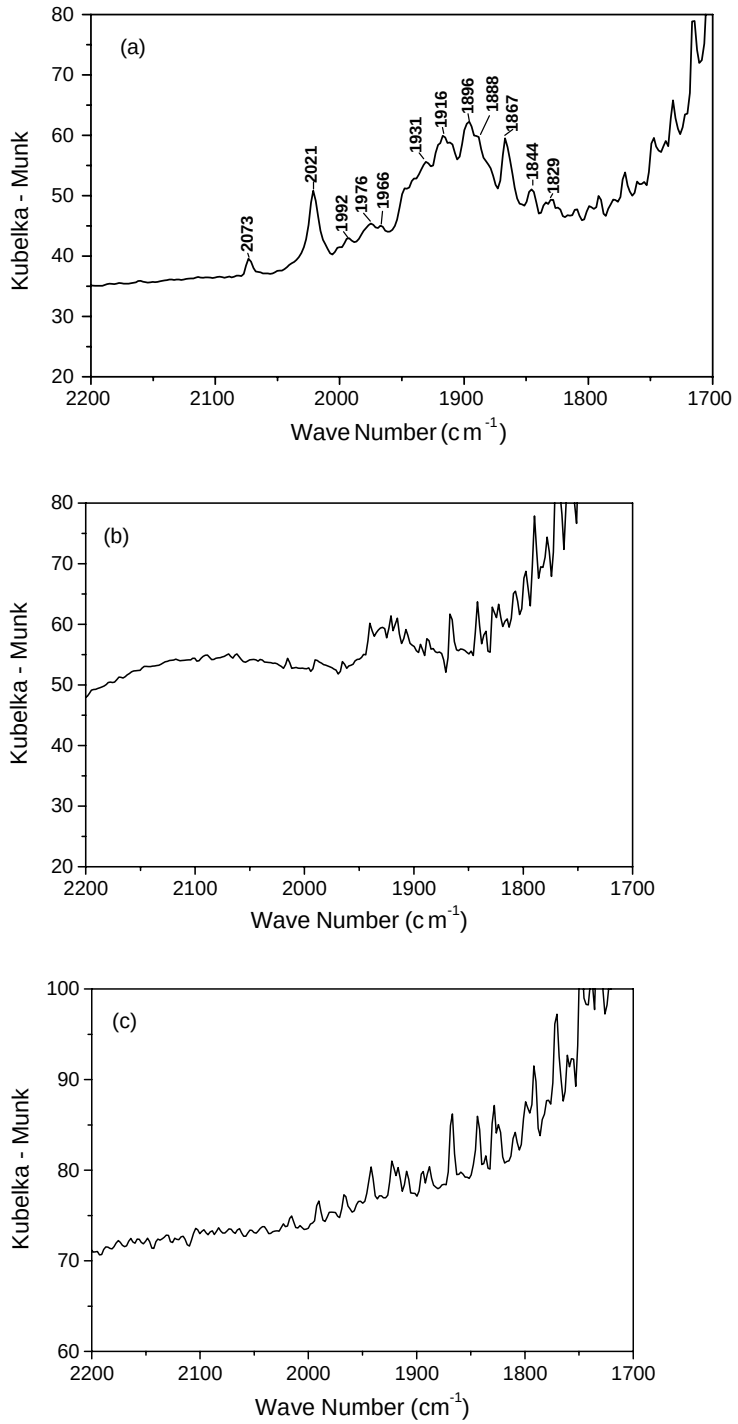


Fig. 3. DRIFTS–FTIR spectra of NaY-zeolite and Pd/NaY (IE); photochemical activation of $[W(CO)_6] + PPh_3$ on NaY-zeolite (a); photochemical activation of $[W(CO)_6]$ on NaY-zeolite (b); photochemical activation of $[W(CO)_6]$ on Pd/NaY (IE) (c).

stronger interaction of M–CO with the Lewis acid sites of the support and a consequent lowering of the symmetry or to different sites for coordination [14]. Examining this spectrum, it can be seen that the bands at 2073 and 1943 $cm^{-1}$ can be attributed to the $a_1$rad and $a_1$ax + e modes, respectively, of the pentacarbonyl derivative $[W(CO)_5PPh_3]$. The band at 2073 $cm^{-1}$ does not change in comparison with that of alumina, but the one around 1943 $cm^{-1}$ is splitted in three, showing that these modes are more sensible to the different interactions with the zeolite acid sites. The bands at 2021, 1916, 1888 and 1867 $cm^{-1}$ are related to $b_2$, $b_1$, $a_1$, e, $a_1$ modes, respectively, of the *cis*-disubstituted compound, *cis*-$[W(CO)_4(PPh_3)_2]$. The weak bands at 1992, 1976 and 1966 $cm^{-1}$ can be related to the $t_{1u}$ mode of $[W(CO)_6]$ interacting in different sites. The band at 1896 $cm^{-1}$ ($e_{1u}$ mode) indicates the presence of the *trans*-disubstituted

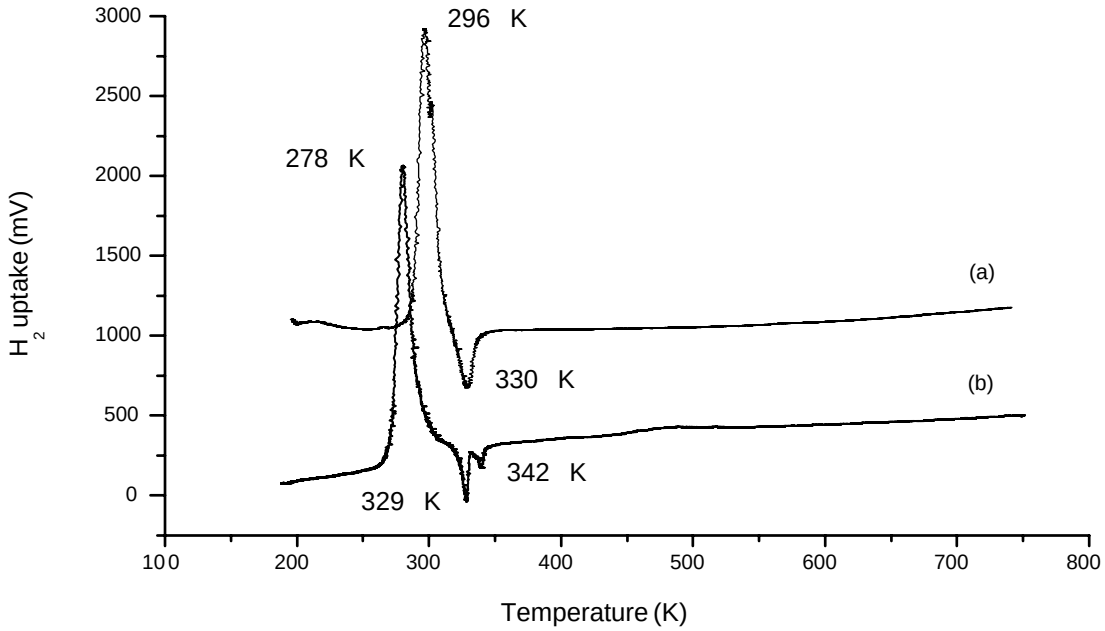


Fig. 4. TPR profiles for Pd-W/NaY (DI), $m = 100$ mg (a) and Pd-W/NaY (IE) $m = 20$ mg (b) following oxidation in $O_2$/Ar at 773 K.

species. In Fig. 3b and c are the spectra obtained in this work for the NaY-zeolite support and the Pd/NaY-zeolite (IE) catalyst without the ligand $PPh_3$. As it can be seen, only traces of $[W(CO)_{6-n}]$ species are observed, because the subcarbonyl species decomposed rapidly upon exposure of the solid sample to air. However, a specific interaction between hexacarbonyl species and the metal surface takes place during the photochemical reaction. Xu and Zaera [28] have shown that a complete and rapid decarbonylation of $[W(CO)_6]$ takes place when this compound is adsorbed on a nickel film. In a previous study we have found evidence that partially decarbonylated species adsorb and decompose rapidly on the surface of reduced palladium [13].

The effect of tungsten addition on the oxidation-reduction behavior of the Pd-W/NaY-zeolite catalysts is shown in Fig. 4. The TPR profile for the Pd-W/NaY (DI)-zeolite sample presents sharp and narrow peaks for hydrogen consumption and hydrogen desorption. The hydrogen consumption peak is positioned at the same temperature shown by the monometallic sample, 296 K, and the calculated peak area demonstrates that despite the change in peak shape the same amount of palladium is involved in the oxidation-reduction process. On the other hand, the hydrogen desorption peak appears at a lower temperature; 330 K. This behavior reflects an interaction between palladium and tungsten that facilitates the decomposition of the β-hydride. The profile for the Pd-W/NaY(IE)-zeolite catalysts reveals a large reduction in hydrogen consumption (about 50%) relative to that of the monometallic catalyst. In addition, the TPR profile exhibits two hydrogen desorption peaks, located at 329 and 342 K. One possible explanation is that the initial sample treatment at 773 K in 5% $O_2$ might be not sufficient to oxidize all Pd atoms due to its interaction with tungsten. The two β-hydride decomposition peaks found for the ionic exchange sample suggests the presence of different palladium particles; large ones with a close interaction with tungsten characterized by a desorption peak at 329 K and small ones located in the α-supercage or the sodalite cage with a desorption at 342 K. Consequently, the TPR measurements demonstrate that both preparation methods lead to a palladium-tungsten interaction. There would appear to be an advantage of using zeolites over alumina, because in our previous studies we have found that tungsten hexacarbonyls have a tendency to interact mainly with large palladium particles supported on alumina [13].

### 3.3. Catalytic activity and selectivity for NO decomposition

#### 3.3.1. Pd/NaY (DI)-zeolite and Pd-W/NaY (DI)-zeolite catalysts

Fig. 5 shows the activity for NO decomposition at 573 K on samples reduced at the same temperature. Both the monometallic and bimetallic catalysts exhibited a period of very high activity followed by a steady deactivation due to oxygen retention by $Pd^{\circ}$ atoms and perhaps $WO_{3-x}$ species formed during the reduction pretreatment. It is generally accepted that the catalytic decomposition of NO occurs on reduced metals. However the oxygen produced by the NO dissociation remains strongly adsorbed and depending on the reaction temperature may even lead to oxidation of the metal. It is shown in Fig. 5 that the bimetallic sample deactivates faster, indicating that, under the chosen conditions, the palladium-tungsten interaction decreased the fraction of exposed palladium atoms. According to these results the addition of tungsten to a Pd/NaY-zeolite catalyst prepared by dry impregnation and containing a moderate

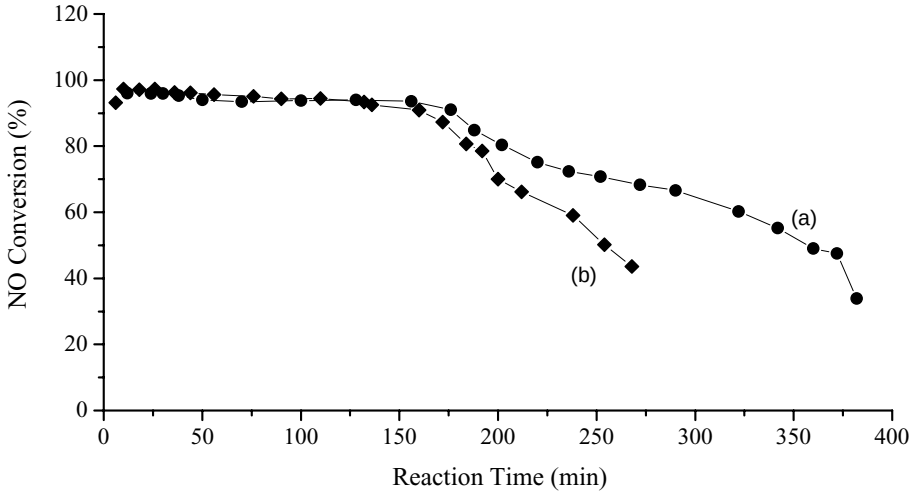


Fig. 5. NO decomposition at 573 K. Conversion (%) vs. time on stream for samples reduced at 573 K. Pd/NaY (DI) (a) and Pd-W/NaY (DI) (b).

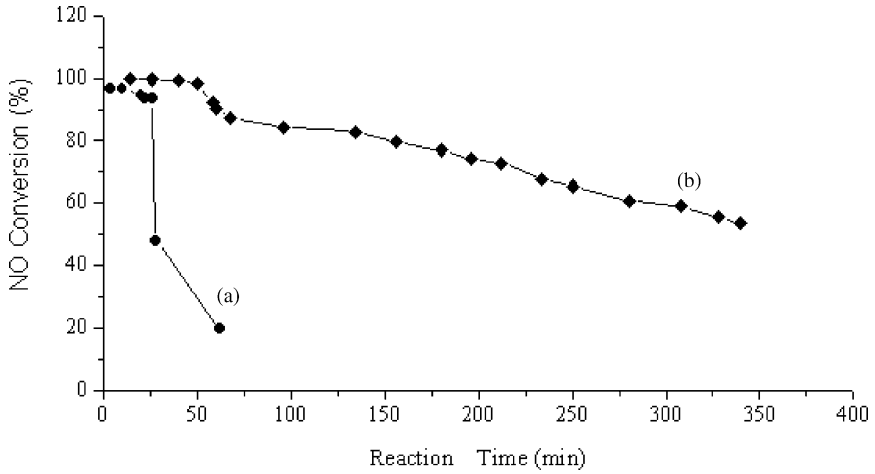


Fig. 6. NO decomposition at 573 K. Conversion (%) vs. time on stream for samples reduced at 973 K. Pd/NaY (DI) (a) and Pd-W/NaY (DI) (b).

palladium loading does not improve its activity for the NO decomposition reaction. As observed in Fig. 6 similar samples reduced at 973 K behave quite differently. In this case, the monometallic catalyst deactivates very rapidly because large palladium particles, with a smaller fraction of exposed metal atoms, are formed by the sintering process that takes place in $H_2$ at 973 K. In other words, the initial $(H/Pd)_s$ ratio ($\geq$0.25) decreases and the 4.5 nm particles growth to some extent. Bulk oxidation of large particles is a slow process that limits the rate of NO decomposition. On the other hand, the presence of tungsten on Pd-W/NaY (DI)-zeolite leads to a brief period of high activity followed by a slow and steady deactivation. The improved behavior of this sample is in part due to the presence of reduced tungsten species and also to inhibition of the palladium sintering process in hydrogen.

In addition to changes in catalytic activity there is a promotional effect of tungsten on the reaction selectivity to $N_2$. It is important to mention first that $N_2O$ and $N_2$ were the only reaction products; the formation of $NO_2$ was negligible. Another characteristic of the NO decomposition reaction on metals observed here was that the onset of $N_2O$ formation is in accord with the initiation of the deactivation process [12]. As shown in Table 2 the presence of tungsten decreases the selectivity to $N_2O$ (for a NO conversion

Table 2
Selectivity to $N_2O$ at 573 K for a NO conversion of 60%

| Catalyst | Reduction temperature (K) | Reaction time (min) | Selectivity[a] to $N_2O$ (%) |
|---|---|---|---|
| Pd/NaY (DI) | 573 | 320 | 81 |
| Pd-W/NaY (DI) | 573 | 238 | 27 |
| Pd/NaY (DI) | 973 | 25 | 17 |
| Pd-W/NaY (DI) | 973 | 300 | 67 |
| Pd/NaY (IE) | 573 | >500 | 87[b] |
| Pd-W/NaY (IE) | 573 | 165 | 60 |
| Pd/NaY (IE) | 973 | 390 | 75 |
| Pd-W/NaY (IE) | 973 | 390 | 52 |

[a] Selectivity to $N_2O = 2 \times$ [ppm $N_2O$]/[ppm NO converted].
[b] Extrapolated value.

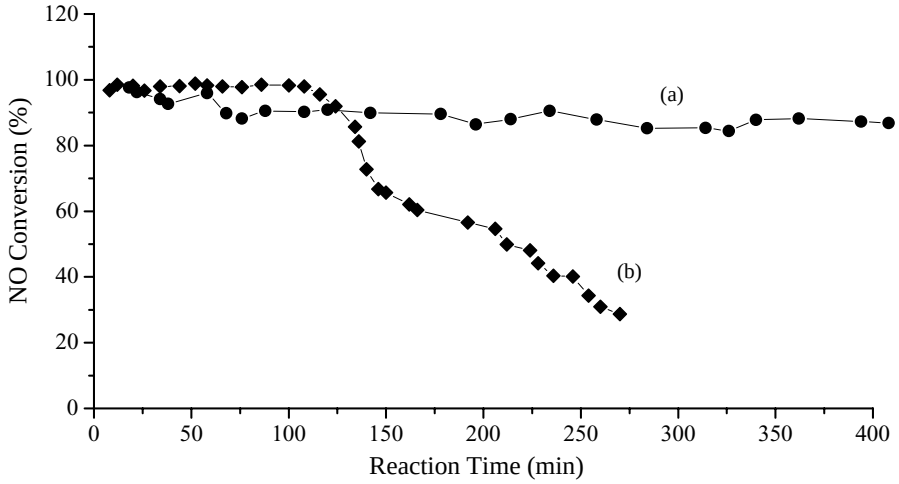


Fig. 7. NO decomposition at 573 K. Conversion (%) vs. time on stream for samples reduced at 573 K. Pd/NaY (IE) (a) and Pd-W/NaY (IE) (b).

of 60%) to a large extent, from 81 to 27% for the Pd/NaY (DI)-zeolite sample reduced at 573 K. It is observed that the reaction time to reach a conversion level of 60% for the bimetallic sample is reduced, in accordance with the loss of activity already discussed. The inhibited formation of $N_2O$ on Pd-W/NaY (DI)-zeolite may be attributed to the resistance of palladium to oxidation or to oxygen retention in the presence of reduced tungsten species, as found on a previous study carried out on Pd-W/$\gamma$-$Al_2O_3$ [29]. It was demonstrated by Rottlander et al. [30] that surface oxygen limits the dissociation of adsorbed NO and consequently the $NO_{ad} + N_{ad}$ reaction is favored. Another interpretation for the change in selectivity may be the promotion of oxygen desorption. It was shown by Chuang and Tan [31] that the addition of terbium oxide to a Pt/$\gamma$-$Al_2O_3$ catalyst facilitates the desorption of oxygen during NO decomposition. Unfortunately, we were not able to follow the evolution of oxygen due to the use of FTIR analysis to follow the reaction progress.

Turning our attention to the behavior of the Pd/NaY (DI)-zeolite sample reduced at 973 K, Table 2 exhibits a sharp decline in activity, 60% conversion in 25 min, but also a very low selectivity to $N_2O$. This is a surprising result because it is expected that large palladium particles favor the formation of $N_2O$ [32]. In our opinion the reason for this behavior is the slow response of the FTIR cell to sudden changes in $N_2O$ concentration. Consequently, the effect of the high reduction temperature on the reaction selectivity of the Pd/NaY (DI)-zeolite sample is apparent.

### *3.3.2. Pd/NaY(IE)-zeolite and Pd-W/NaY(IE)-zeolite catalysts*

The monometallic sample exhibited a high and stable activity for a period of 7 h when reduced at 573, as shown in Fig. 7. When tungsten was incorporated there was a period of 100% conversion of approximately 100 min followed by a marked deactivation. Therefore, here again it seems that the presence of tungsten in close association with palladium

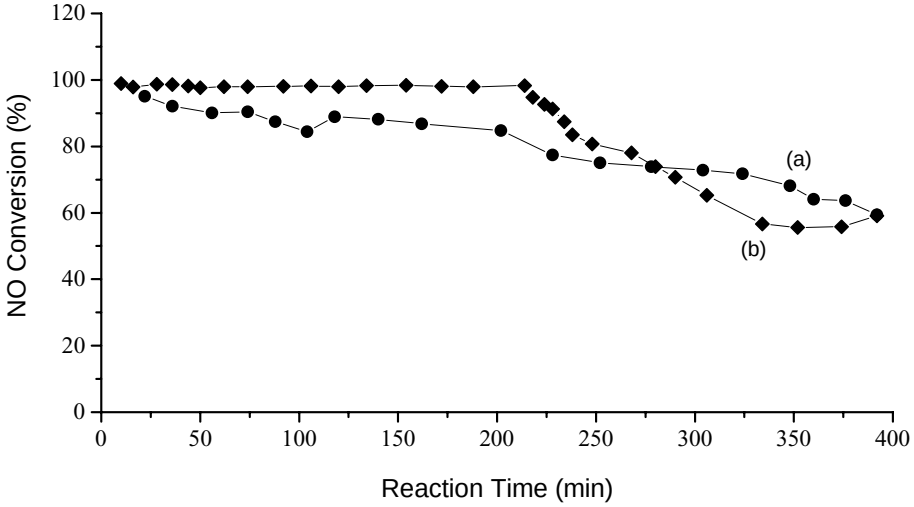


Fig. 8. NO decomposition at 573 K. Conversion (%) vs. time on stream for samples reduced at 973 K. Pd/NaY (IE) (a) and Pd-W/NaY (IE) (b).

particles inhibited the NO reaction. However, when the reduction temperature was 973 K, a more comparable performance between the mono and the bimetallic catalyst was obtained. As observed in Fig. 8 the Pd-W/NaY(IE)-zeolite catalysts exhibited a conversion of 100% for about 3 h, followed by a slow deactivation. This behavior is attributed to the presence of reduced tungsten species. No change in palladium particle size should be expected, because of the very large particles on the fresh catalyst obtained by the IE preparation method.

Turning the attention to the reaction selectivity, the beneficial effect of tungsten addition on catalysts prepared by IE was important for samples reduced at 573 and 773 K. The results in Table 2 indicate a clear reduction on the undesirable formation of $N_2O$; the selectivity to this compound decreased from 87 to 60% and from 75 to 52% depending on the reduction temperature. Here again several interpretations could be offered to explain these results; the presence of reduced tunsgten species may act as oxygen scavenger or may facilitate the desorption of oxygen. More specific studies are needed to discriminate between these possibilities.

## 4. Conclusions

It has been demonstrated that the photochemical reaction of tungsten hexacarbonyl with Pd/NaY-zeolite catalysts of high (large particles) and low (small particles) metal content enables the preparation of bimetallic samples. The method of preparation leads to a palladium-tungsten interaction that modifies the catalytic activity and the selectivity of the Pd/NaY-zeolite catalysts for the NO decomposition reaction. For samples reduced at high temperature, the presence of tungsten prevents the sintering of small palladium particles. However, the main effect of tungsten is a reduction on the selectivity to $N_2O$. In other words, tungsten suppresses the undesirable formation of $N_2O$.

## Acknowledgements

The authors acknowledge the financial support provided by CNPq (Brazil), FAPERGS (Brazil), COPESUL (Brazil), CONICET (Argentina) and to Dr. John Spencer (John Black foundation, England) for proof reading this article.

## References

[1] H.S. Ghandi, H.C. Yao, H.K. Stepien, in: A.T. Bell, L.L. Hegedus (Eds.), Catalysis Under Transient Conditions, A.C.S. Symposium Series, 1982, 178, p. 143.
[2] K.M. Adams, H.R. Ghandi, Ind. Eng. Chem. Prod. Res. Dev. 22 (1983) 207.
[3] H.K. Plummer, S. Shinozaki, K.M. Adams, H.S. Ghandi, J. Mol. Catal. 20 (1983) 251.
[4] H. Muraki, H. Shinjoh, H. Sobukawa, K. Yokota, Y. Fujitani, Ind. Eng. Chem. Res. Dev. 25 (1986) 202.
[5] I. Halasz, A. Brenner, M. Shelef, K.Y. Simon Ng, Appl. Catal. A 82 (1992) 51.
[6] I. Halasz, A. Brenner, M. Shelef, Appl. Catal. B 2 (1993) 31.
[7] T. Sekiba, S. Kimura, H. Yamamoto, A. Okada, Catal. Today 22 (1994) 113.
[8] Y.J. Mergler, A. Van Aalst, J. van Delft, B.E. Nieuwenhuys, J. Catal. 161 (1996) 310.
[9] M.A.S. Baldanza, L.F. de Melo, A. Vannice, F.B. Noronha, M. Schmal, J. Catal. 192 (2000) 64.
[10] I.M. Baibich, J.H. dos Santos, F. Stedile, V.E. Santarosa, I. Baumvol, Polyhedron 16 (11) (1997) 1937.
[11] I.M. Baibich, J.H. dos Santos, V.C. da Silveira, C.E. Gigola, A.M. Sica, Canadian J. Anal. Sci. Spectrosc. 43 (1) (1998) 26.
[12] A.M. Sica, J.H. dos Santos, I.M. Baibich, C.E. Gigola, J. Mol. Catal. A 137 (1999) 287.
[13] A.M. Sica, I.M. Baibich, C. Gigola, J. Mol. Catal. A 195 (2003) 225.
[14] R.M.J. de Almeida, S.B.C. Pergher, C.E. Gigola, I.M. Baibich, Canadian J. Anal. Sci. Spectrosc. 48 (1) (2003) 21.
[15] R.M. Dallago, PhD Thesis, Instituto de Química, UFRGS, Brazil, 2002.
[16] S. Özar, G.A. Ozin, K. Moller, T. Bein, J. Am. Chem. Soc. 112 (26) (1990) 9575.
[17] G.A. Ozin, S. Özar, H.O. Pastore, A.J. Pöe, E.J.S. Vichi, J. Chem. Soc. Chem. Commun. (1991) 141.
[18] R. Jelinek, S. Özar, H.O. Pastore, A. Malek, G.A. Ozin, J. Am. Chem. Soc. 115 (1993) 563.
[19] H.O. Pastore, G.A. Ozin, A.J. Pöe, J. Am. Chem. Soc. 115 (1993) 1215.
[20] C.J. Loughran, D.E. Resasco, Appl. Catal. B 7 (1995) 113.
[21] C. Descorme, P. Gélin, C. Lécuyer, M. Primet, J. Catal. 177 (1998) 352.
[22] P. Cañizares, A. de Lucas, F. Dorado, A. Durán, I. Asencio, Appl. Catal. A 169 (1998) 137.
[23] J.L. Benson, H.S. Hwang, M. Boudart, J. Catal. 30 (1973) 146.
[24] R.M. Dallago, J. Schifino, I.M. Baibich, R.C. Vezes, PhD Thesis, Instituto de Química, Universidade Federal do Rio Grande do Sul, 2002.
[25] S. Ichikawa, H. Poppa, M. Boudart, J. Catal. 91 (1985) 1.
[26] S.T. Homeyer, W.M.H. Sachtler, Appl. Catal. 54 (1989) 189.
[27] M. Boudart, H.S. Hwang, J. Catal. 39 (1975) 44.
[28] M. Xu, J. Zaera, J. Vac. Sci. Technol. A 14 (1996) 415.
[29] A.M. Sica, C.E. Gigola, Appl. Catal. A 239 (1–2) (2003) 121.
[30] C. Rottlander, R. Andorf, C. Plog, B. Krutzsch, M. Baerns, J. Catal. 169 (1997) 400.
[31] S.S.C. Chuang, Cher-Dip Tan, J. Phys. Chem. B 101 (1997) 3000.
[32] X. Xu, D.W. Goodman, Catal. Lett. 24 (1994) 31.